JOURNAL OF SOLID STATE CHEMISTRY **134,** 170–181 (1997)
ARTICLE NO. SC977572

Cation Distribution in Ordered Spinels of the Li_2O–TiO_2–Fe_2O_3 System

S. Scharner[1] and W. Weppner

Lehrstuhl für Sensorik und Festkörperionik, Technische Fakultät der Christian-Albrechts-Universität zu Kiel, Kiel, D-24143, Germany

and

P. Schmid-Beurmann

Mineralogisch Petrographisches Institut, Christian-Albrechts-Universität zu Kiel, Kiel, D-24098, Germany

Received March 17, 1997; in revised form July 28, 1997; accepted July 29, 1997

Several solid solutions of $Li_{0.5+0.5x}Fe_{2.5-1.5x}Ti_xO_4$ type synthesized at 870°C in oxygen and slowly cooled to room temperature were investigated by X-ray powder diffractometry and ^{57}Fe-Mössbauer spectroscopy. In the ranges $0 \le x \le 0.4$ and $1.2 \le x \le 1.57$ the compounds crystallize in the space group $P4_332$, whereas the ideal spinel structure with space group $Fd\bar{3}m$ is obtained in the ranges $0.4 \le x \le 1.2$ and $1.57 \le x \le 1.66$. Site occupancies were calculated from the refined scattering factors of the metal sites using the Rietveld method, revealing strong ordering of lithium on the octahedral sites (4*b*) of the space group $P4_332$ for compounds between $1.2 \le x \le 1.57$. With the help of ^{57}Fe-Mossbauer data of titanium–rich compounds and literature data, the site distribution of Li^+, Fe^{3+}, and Ti^{4+} for the whole compositional range was calculated, indicating a redistribution of Fe and Li on the octahedral and tetrahedral positions when passing the phase transition at $x = 1.57$ toward higher titanium contents. The compositional dependancy of the lattice parameter *a* shows a sigmoidal behavior in the region $1.2 \le x \le 1.57$ which was correlated with this intracrystalline order–disorder process.

INTRODUCTION

The lithium titanate spinel $Li_{1.33}Ti_{1.66}O_4$ has been proposed as an electrode material for rechargable lithium batteries (1–3). During the charging process, insertion of lithium changes the initially white compound reversibly to deep blue. Materials with this property are called electrochromic and can be used as thin film electrodes in light modulating devices, such as windows, mirrors, safety glasses or even electrochromic displays. Two electrodes and an electrolyte are needed to build an electrochromic device (4). At least one of the electrodes must be electrochromic while the other may stay transparent. While the pure lithium titanate spinel $Li_{1.33}Ti_{1.66}O_4$ may be used as an electrochromic electrode, iron-substituted lithium titanates with a spinel structure may be interesting counter-electrode materials.

Most of the previous publications concerning the $Li_{1.33}Ti_{1.66}O_4$–$Li_{0.5}Fe_{2.5}O_4$ spinel join deal with the iron compounds, less attention has been given to the titanium-rich phases. The aim of this article is to close this gap. It will be shown how X-ray diffraction in combination with the Rietveld method and ^{57}Fe-Mössbauer spectroscopy can be used to solve the problem of the cation ordering in the mixed-cation spinel system. Precise lattice constants will also be given.

PREVIOUS WORK

The iron-rich compounds of the $Li_{1.33}Ti_{1.66}O_4$–$Li_{0.5}Fe_{2.5}O_4$ spinel system have been the subject of many investigations that deal with their magnetic properties and cationic distribution between tetrahedral *A* and octahedral *B* sites (5–16).

The widely accepted model of site distribution of the spinel solid solution system with the general formula $(Fe_{1-0.5x}Li_{0.5x})_A(Fe_{1.5-x}Li_{0.5}Ti_x)_BO_4$ was already derived by Blasse and later confirmed by Noguès *et al.* (5, 7). However, this formula is only valid from stoichiometrical and structural reasons for compounds with $x \le 1.50$ which crystallize in the space group $Fd\bar{3}m$, where all octahedral (16*d*) sites are symmetrically equivalent. It was already reported by Blasse (5), but never confirmed by other authors, that slowly cooled spinels of the iron-rich side ($0 \le x \le 0.33$) as well as titanium-rich compositions ($1.22 \le x \le 1.56$) are isotypic with the endmember $Li_{0.5}Fe_{2.5}O_4$ ($x = 0$). At low temperatures $Li_{0.5}Fe_{2.5}O_4$ crystallizes in an ordered form of the spinel structure with the space group $P4_332$ (17, 18). The

[1] To whom correspondence should be addressed.

0022-4596/97 $25.00

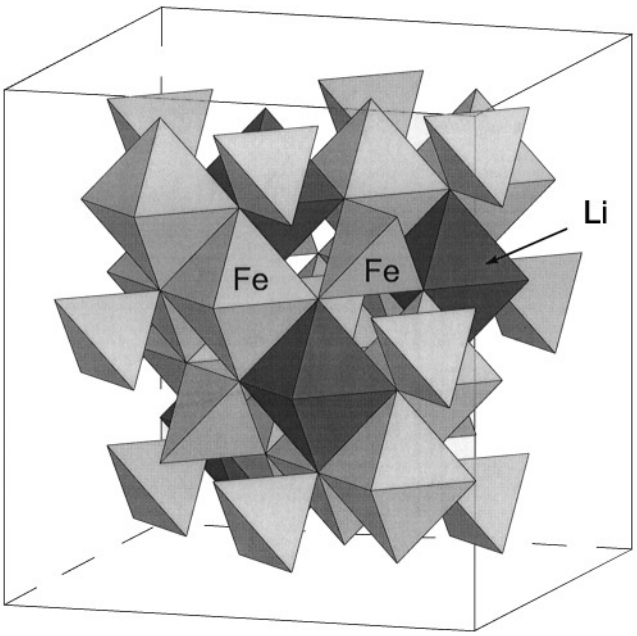

FIG. 1. The crystal structure of the ordered low-temperature modification of $Li_{0.5}Fe_{2.5}O_4$ with the space group $P4_332$ (17, 18). The edge-sharing octahedra form infinite chains which are occupied by Li^+ (dark polyhedra) and Fe^{3+} (bright polyhedra). Octahedra and FeO_4 tetrahedra share common vertices.

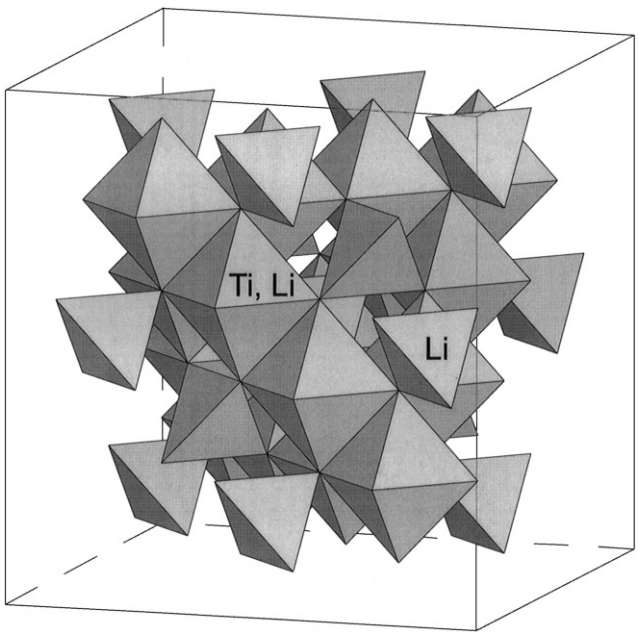

FIG. 2. The structure of $Li_{1.33}Ti_{1.66}O_4$ (20). The octahedra forming infinite chains are randomly occupied by Li^+ and Ti^{4+}. Octahedra and LiO_4 tetrahedra share common vertices.

octahedral (12*d*) and tetrahedral (8*c*) sites are completely occupied by iron, whereas the octahedral (4*b*) sites are occupied by lithium (Fig. 1). At temperatures between 735 and 755°C $Li_{0.5}Fe_{2.5}O_4$ undergoes an order–disorder phase transition from space group $P4_332$ to space group $Fd\bar{3}m$ (19).

$Li_{1.33}Ti_{1.66}O_4$ crystallizes in space group $Fd\bar{3}m$ with the octahedral (16*d*) sites statistically occupied by lithium and titanium, whereas the tetrahedral (8*c*) positions are occupied by lithium (20). The structure of $Li_{1.33}Ti_{1.66}O_4$ is shown in Fig. 2.

EXPERIMENTAL TECHNIQUES

Synthesis

Stoichiometric amounts of Li_2CO_3 (Merck, puriss.), TiO_2 (Anatase, Aldrich 99.9 + %), and Fe_2O_3 (Alfa, 99.9%) were used. All starting materials were dried and checked for phase purity by X-ray diffraction before use. After ball milling with zirconia cups and balls, the lubricating alcohol was evaporated and the homogenized mixtures were fired in a single-step process at 750°C for 12 h and at 870°C for 24 h in a quartz-tube furnace using Alsint crucibles (Haldenwanger, Berlin). The heating and cooling rates (60°C/h) were controlled by an Eurotherm 902P programmable temperature controller equipped with a Chromel–Alumel thermocouple. The temperature gradient within the sample was less than 5°C at 870°C. During the reaction process a constant flux of pure oxygen (AGA 5.0) of 100 sccm was maintained using a Tylan FC280 mass flow controller to minimize reduction of the Fe^{3+}. The reaction products were ground in an agate mortar and stored in a dry dessicator loaded with P_4O_{10}.

X-Ray Powder Diffraction

Powder diffractograms for phase analysis and Rietveld refinement were recorded using a Seifert XRD 3000 system with fixed sample configuration in the Bragg–Brentano geometry and conditions of Table 1. The instrument was equipped with a secondary curved graphite monochromator separating diffracted Cu$K\alpha$ radiation with the wavelengths 1.540598 and 1.544426 Å. Powders were ground in an agate mortar and filled into polyvinyl sample holders, smoothed by a microscopy glass substrate giving layers with 1.5×2.6 cm surface and 0.7 mm thickness, and then fixed in the standard sample holder of the instrument.

The lattice constants were determined from X-ray powder diffractions recorded with a Siemens D5000 diffractometer and 15 wt% of silicon (NBS 640b) as internal standard (Table 1). The line positions were determined by fitting

TABLE 1
Conditions for X-Ray Powder Data Collection for Rietveld Refinement and Lattice Constant Determination

	Rietveld refinement	Lattice constant determination
Diffractometer	Seifert XRD 3000 (θ/θ)	Siemens D5000 ($\theta/2\theta$)
Radiation	Cu$K\alpha$	Cu$K\alpha$
Radius	250 mm	250 mm
Monochromator	secondary	secondary
Current/voltage	30 mA/40 kV	25 mA/40 kV
2θ-range (°)	14–100	15–160
Step size (°)	0.01	0.02
Measuring time/step	12 s	6 s
Mode	step scan	step scan
Soller slits	primary and secondary	primary
Primary divergency slit	fixed (0.3°)[a]	variable *V6*
Secondary divergency slit	none	fixed (3°)[a]
Detector slit	1.0 mm	0.6 mm
Internal standard	none	15 w% Si NBS 640b

[a] Aperture angle.

a Split-Pearson profile function to each reflection considering Cu$K\alpha_2$ radiation. The unit-cell constants were then refined using the least-squares program PULVER91 (Weber, 1991).

Mössbauer Spectroscopy

^{57}Fe-Mössbauer spectra were recorded at 78 K absorber temperature using conventional techniques. The ^{57}Co/Rh (ca 1.85 GBq) source was kept at room temperature. The sample (5 mg Fe/cm^2 absorber density with an avicel matrix) was moved with constant acceleration and symmetric triangular wave form. The velocity was calibrated using an α-Fe foil.

Rietveld Analysis

The refinements were performed using the Rietveld program package WYRIET, Version 3 (M. Schneider EDV Vertrieb, D-82343 Pöcking, Germany). Data from 14° to 100° (2θ) with a resolution of 0.01° (2θ) were included into the calculation (Table 1). The nonatomic variables refined were: zero correction, scale factor, two mixing parameters of the pseudo-Voigt line profile, a line asymmetry parameter, three halfwidth parameters, and the unit-cell parameter. The background was fitted by hand using the program BAPL from the WYRIET program package.

THEORETICAL ASPECTS

Site Occupancy Derivation

The cationic distribution was determined from the refined scattering factors of the metal sites from Rietveld analysis with the following approximations and external conditions:

I. the approximate proportionality of the mean atomic scattering factors of Li^+, Ti^{4+}, and Fe^{3+} with diffraction angle.

II. the full occupancy of the cationic sites.

III. the known titanium content of the samples.

IV. the samples were treated as single-phased and small amounts, e.g., about 1% of rutile, were neglected.

IV. During Bragg diffraction, the amplitude F_{hkl} is given by

$$F_{hkl} = \sum_{j=1}^{n} S_j \cdot e^{2\pi i(hx_j + ky_j + lz_j)} \cdot e^{-B_j \cdot \sin^2\theta/\lambda^2}, \qquad [1]$$

where S_j is the scattering factor, x_j, y_j, z_j are the positional coordinates, and B_j is the isotropic temperature factor of the jth site in the asymmetric unit. If a lattice site j is occupied by more than one chemical species i, S_j equals the sum of the products of the mean atomic scattering factors f_i and their site occupancy multipliers N_i^j (21)

$$S_j = \sum_i f_i \cdot N_i^j. \qquad [2]$$

N_i^j is defined as the fractional site occupancy (100% denotes full occupancy) of an individual species multiplied by the multiplicity of the actual site j and divided by the multiplicity of the general position of the space group (22).

The ordered spinels with formula $Li_{0.5+0.5x}Fe_{2.5-1.5x}Ti_xO_4$ in the compositional range $1.2 \leq x \leq 1.57$ crystallize in the space group $P4_332$. This space group provides three different lattice sites, octahedral (4*b*) and (12*d*) as well as tetrahedral (8*c*) sites which can be occupied by the different cations. For this special case, nine site occupancy multipliers must be determined. However, the exact site distribution cannot be derived from a powder diffraction experiment (21). Instead, the range of physically reasonable solutions may be approximated using the external conditions I to IV and the procedure which will be described in the following.

The approximate proportionality of the atomic scattering factors of Li^+, Ti^{4+}, and Fe^{3+} with diffraction angle in the 2θ range from 0° to 100° (2θ), can be taken from Fig. 3. The ratios of the atomic scattering factors are approximately independent from the diffraction angle 2θ:

$$a = \frac{f_{Ti^{4+}}}{f_{Fe^{3+}}} = 0.79(1) \quad \text{and} \quad b = \frac{f_{Li^+}}{f_{Fe^{3+}}} = 0.088(1). \qquad [3]$$

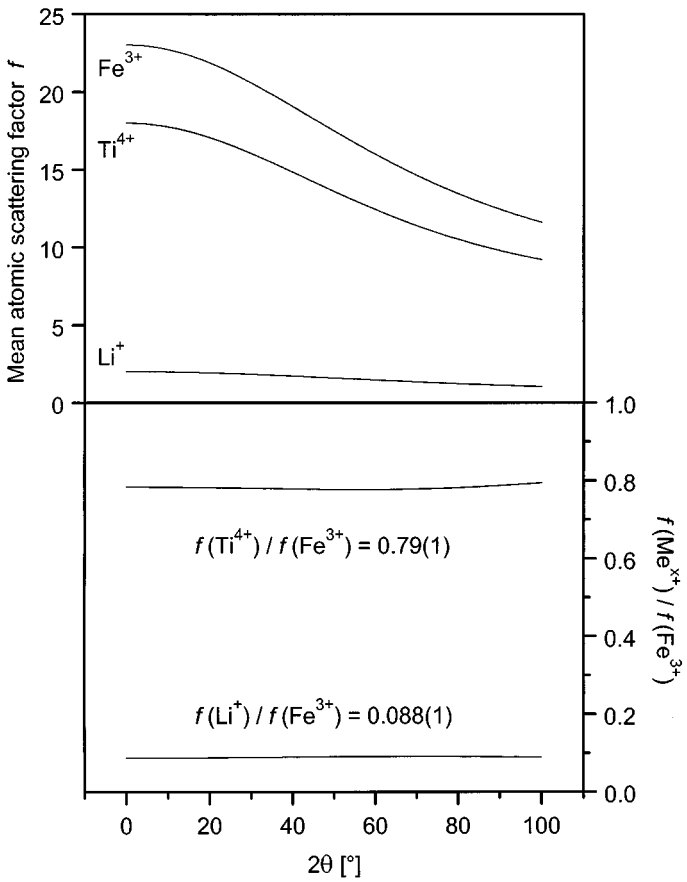

FIG. 3. Mean atomic scattering factors f (Cu$K\alpha$ radiation) of the ions Li^+, Ti^{4+}, and Fe^{3+} between 0° and 100° in 2θ (23). The ratios $f_{Li^+}/f_{Fe^{3+}}$ and $f_{Ti^{4+}}/f_{Fe^{3+}}$ are approximately constant and demonstrate the proportionality between these scattering factors.

Equation [2] must be written as

$$S_j = \sum_i f_i \cdot N_i^j = f_{Ti^{4+}} N_{Ti^{4+}}^j + f_{Fe^{3+}} N_{Fe^{3+}}^j + f_{Li^+} N_{Li^+}^j. \quad [4]$$

The coefficients a and b from [3] can be used to replace two of the scattering factors f_i for the third. We have done this for f_{Li^+} and $f_{Ti^{4+}}$

$$S_j \approx a \cdot f_{Fe^{3+}} . N_{Ti^{4+}}^j + f_{Fe^{3+}} \cdot N_{Fe^{3+}}^j + b \cdot f_{Fe^{3+}} \cdot N_{Li^+}^j \quad [5]$$

$$S_j \approx (a \cdot N_{Ti^{4+}}^j + N_{Fe^{3+}}^j + b \cdot N_{Li^+}^j) \cdot f_{Fe^{3+}} = C^j \cdot f_{Fe^{3+}}. \quad [6]$$

Within the limits of the approximation [3] the atomic scattering factors S_j of the cationic lattice sites (4*b*), (12*d*), and (8*c*) may be described by the product of a single atomic scattering factor $f_{Fe^{3+}}$ and a constant parameter C^j. The C^j's may be determined from a Rietveld refinement procedure when filling up each lattice site with the same cation, here Fe^{3+}. The refinement yields the site occupancy multipliers which we have denoted as C^{4b}, C^{12d}, and C^{8c}, e.g., Tables 2 and 3.

From Eq. [6] we obtain three equations to determine the N_i^j

$$a \cdot N_{Ti^{4+}}^{12d} + N_{Fe^{3+}}^{12d} + b \cdot N_{Li^+}^{12d} = C^{12d} \quad [7]$$

$$a \cdot N_{Ti^{4+}}^{4b} + N_{Fe^{3+}}^{4b} + b \cdot N_{Li^+}^{4b} = C^{4b} \quad [8]$$

$$a \cdot N_{Ti^{4+}}^{8c} + N_{Fe^{3+}}^{8c} + b \cdot N_{Li^+}^{8c} = C^{8c}. \quad [9]$$

Three additional equations may be derived using assumption II (full site occupancy):

$$N_{Ti^{4+}}^{4b} + N_{Fe^{3+}}^{4b} + N_{Li^+}^{4b} = \tfrac{1}{6} \quad [10]$$

$$N_{Ti^{4+}}^{12d} + N_{Fe^{3+}}^{12d} + N_{Li^+}^{12d} = \tfrac{1}{2} \quad [11]$$

$$N_{Ti^{4+}}^{8c} + N_{Fe^{3+}}^{8c} + N_{Li^+}^{8c} = \tfrac{1}{3}. \quad [12]$$

1/6, 1/2, and 1/3 are the values of the site occupancy multipliers when the Wyckoff positions (4*b*), (12*d*), and (8*c*) of the space group $P4_332$ are fully occupied.

Finally, the last three conditional equations may be derived when the composition of a sample is known

$$N_{Ti^{4+}}^{4b} + N_{Ti^{4+}}^{12d} + N_{Ti^{4+}}^{8c} = x/3 \quad [13]$$

$$N_{Fe^{3+}}^{4b} + N_{Fe^{3+}}^{12d} + N_{Fe^{3+}}^{8c} = (2.5 - 1.5 \cdot x)/3 \quad [14]$$

$$N_{Li^+}^{4b} + N_{Li^+}^{12d} + N_{Li^+}^{8c} = (0.5 + 0.5 \cdot x)/3. \quad [15]$$

In Eqs. [13]–[15] x is the parameter in the formula $Li_{0.5+0.5x}Fe_{2.5-1.5x}Ti_xO_4$. From the resulting set of nine conditional equations used to determine the N_i^j only seven (Eqs. [7]–[13]) are independent of each other. Consequently, two of the nine unknown N_i^j remain undetermined and must be treated as variables (we have chosen $N_{Fe^{3+}}^{12d}$ and $N_{Fe^{3+}}^{8c}$). In order to find all physical reasonable sets of site occupancy multipliers, $N_{Fe^{3+}}^{12d}$ and $N_{Fe^{3+}}^{8c}$ were systematically varied between zero and the value for full-site occupancy. All other site occupancy multipliers were then calculated using Eqs. [7]–[13]. Physically insignificant sets of solutions, characterized by one or more negative values of any site occupancy multiplier were then eliminated. With this kind of approximation calculus we were able to find solutions for the distribution of cations among the available crystallographic positions. The calculation of the cationic distribution of the solid solution members with the space group $Fd\bar{3}m$ was done in a similar manner.

TABLE 2
Structural and Cell Parameters of $Li_{0.5}Fe_{2.5}O_4$ and $Li_{1.19}Fe_{0.42}Ti_{1.39}O_4$ from the Rietveld Refinement

		$Li_{0.5}Fe_{2.5}O_4$[a] single crystal	$Li_{0.5}Fe_{2.5}O_4$ powder		$Li_{0.5}Fe_{2.5}O_4$ powder	$Li_{1.19}Fe_{0.42}Ti_{1.39}O_4$ powder
		Comparison with literature data			Refinement of scattering factors	
Space group Wyckoff position		$P4_332$ Scattering factors of Li^+ and Fe^{3+} used			$P4_332$ Scattering factor of Fe^{3+} used for all metal sites	
		Li	Li		$f(Fe^{3+})$	$f(Fe^{3+})$
4*b*	$x=y=z$	5/8	5/8	$x=y=z$	5/8	5/8
	N	1/6	0.142(4)	C^{4b}	0.0130(4)	0.0158(3)
		Fe	Fe		$f(Fe^{3+})$	$f(Fe^{3+})$
12*d*	x	1/8	1/8	x	1/8	1/8
	y	0.3674(1)	0.3661(1)	y	0.3661(1)	0.3667(1)
	z	$1/4-y$	$1/4-y$	z	$1/4-y$	$1/4-y$
	N	1/2	0.504(2)	C^{12d}	0.503(2)	0.415(2)
		Fe	Fe		$f(Fe^{3+})$	$f(Fe^{3+})$
8*c*	$x=y=z$	−0.0023(1)	−0.0036(1)	$x=y=z$	−0.0036(1)	−0.0024(2)
	N	1/3	0.337(1)	C^{8c}	0.337(1)	0.1188(4)
		O1	O1		O1	O1
8*c*	$x=y=z$	0.3853(3)	0.3869(4)	$x=y=z$	0.3868(4)	0.3900(3)
	N	1/3	1/3	N	1/3	1/3
		O2	O2		O2	O2
24*e*	x	0.1166(3)	0.1177(4)	x	0.1177(4)	0.1087(3)
	y	0.1284(3)	0.1268(3)	y	0.1268(3)	0.1249(2)
	z	0.3853(3)	0.3806(3)	z	0.3806(3)	0.3893(2)
	N	1/1	1/1	N	1/1	1/1
	$B_{overall}$ [Å^2]		0.29(2)		0.29(2)	0.73(2)
	a [Å]	8.314(3)	8.33003(8)		8.33003(8)	8.35552(7)
Number of profile points			8601		8601	8601
Number of independent reflections			82		82	84
Number of refined parameters			18		18	18
$R_{wp}=100\{\sum w(y_{obs}-y_{cal})^2/\sum wy_{obs}^2\}^{1/2}$			8.84		8.85	8.79
$R_p=100\{\sum\lvert y_{obs}-y_{cal}\rvert/\sum\lvert y_{obs}\rvert\}$			6.21		6.21	6.26
$R_{exp}=100\{(N-P)/\sum wy_{obs}^2\}$			5.74		5.74	5.57
$R_{Bragg}=100\sum\lvert I_o-I_c\rvert/\sum I_o$			4.62		4.70	4.95
R_{wp}/R_{exp} (Goodness of fit)			1.54		1.54	1.58

Note. C^j, according to Eqs. [6]–[9].
[a] From Ref. (17).

RESULTS

Characterization of the $Li_{1.33}Ti_{1.66}O_4$–$Li_{0.5}Fe_{2.5}O_4$ Spinel Phases

Several X-ray powder diffractograms of the solid solution system $Li_{0.5}Fe_{2.5}O_4$ (*ss*) are shown in Fig. 4. According to Blasse (5) the whole system is classified by two different sets of X-ray diffractions (5). The first set of diffractograms is of $Li_{1.33}Ti_{1.66}O_4$ type with $0.55 \le x \le 1.11$ or $1.59 \le x \le 1.66$. Herein, all reflections can be indexed using the extinction laws of the space group $Fd\bar{3}m$. The second set of diffractograms is of $Li_{0.5}Fe_{2.5}O_4$ type. Diffractograms of this group belong to compositions either rich in iron, $0 \le x \le 0.33$, or rich in titanium, $1.22 \le x \le 1.56$. This set of diffractograms is characterized by additional reflections with regard to the first set and can be assigned to the space group $P4_332$.

Figure 5 shows the composition dependent disappearance of the additional reflections typical for compounds with space group symmetry $P4_332$ when approaching the phase transition border. At $x \approx 1.39$ these reflections show a maximum in intensity with the line widths being as narrow as those reflections common to both space groups. Close to the boundary of the $Li_{1.33}Ti_{1.66}O_4$-type patterns the intensity of the extra lines decreases and a strong line broadening

TABLE 3
Structural and Cell Parameters of $Li_{1.33}Ti_{1.66}O_4$ and $LiFeTiO_4$ from the Rietveld Refinement at Room Temperature

		$Li_{1.33}Ti_{1.66}O_4$[a] single crystal	$Li_{1.33}Ti_{1.66}O_4$ powder		$Li_{1.33}Ti_{1.66}O_4$ powder	$LiFeTiO_4$ powder
		Comparison with literature data			Refinement of scattering factors	
Space group		$Fd\bar{3}m$			$Fd\bar{3}m$	
Wyckoff position		Scattering curve of Li^+ and Ti^{4+} used for metal sites			Scattering curve of Fe^{3+} used for all metal sites	
		Li	Li		$f(Fe^{3+})$	$f(Fe^{3+})$
8*a*	$x=y=z$	0	0	$x=y=z$	0	0
	N	1/24 = 0.0417	0.0404(5)[b]	C^{8a}	0.0037(1)	0.0234(1)
		Li	Li		$f(Fe^{3+})$	$f(Fe^{3+})$
16*d*	$x=y=z$	5/8	5/8	$x=y=z$	5/8	5/8
	N	0.0139	0.0140(5)[b]	C^{16d}	0.0573(2)	0.0566(3)
		Ti	Ti			
16*d*	$x=y=z$	5/8	5/8			
	N	0.069	0.0690(2)			
		O	O		O	O
32*e*	$x=y=z$	0.389	0.3881(1)	$x=y=z$	0.3882(1)	0.3847(1)
	N	1/6	1/6	N	1/6	1/6
	$B_{overall}$ [Å^2]		0.93(2)		0.79(2)	0.83(3)
	a [Å]	8.357	8.35894(8)		8.35893(8)	8.3567(1)
Number of profile points			8601		8601	8601
Number of independent reflections			24		24	24
Number of refined parameters			12		12	12
R_{wp}			8.53		8.62	10.25
R_p			5.56		5.69	7.11
R_{exp}			4.36		4.35	8.53
R_{Bragg}			2.10		2.40	1.93
R_{wp}/R_{exp}			1.95		1.98	1.20

[a] Single crystal data from from Ref. (20).
[b] These parameters were constrained in order to keep the lithium content constant.

is apparent. In contrast to this the line width of all common reflections is independent from composition, see Fig. 6 for example. The line broadening can be explained by assuming that the size of the ordered domains inside the crystallites decreases below the size which is necessary for the production of sharp Bragg reflections.

No support was found for a miscibility gap in the iron-rich part of our samples prepared at 870°C and then slowly cooled. For samples quenched from 755°C and below Yau and Hughes proposed a miscibility gap between $0.05 \leq x \leq 0.6$ (24). As diagnostic feature for the presence of a miscibility gap we used the line width of the Bragg reflections whereas Yau and Hughes did not give an explanation for their conclusion. Samples within such a gap would contain two compositionally different members of the $Li_{1.33}Ti_{1.66}O_4$–$Li_{0.5}Fe_{2.5}O_4$ join. This should result in line broadening or peak splitting. However, our measurements of the full width at half maximum (FWHM) of the common reflection (159) did not indicate any significant line broadening in samples with $x = 0.11$, 0.33, and 0.56 (Fig. 6).

Cationic Site Distribution in the $Li_{0.5}Fe_{2.5}O_4$–$Li_{1.33}Ti_{1.66}O_4$ Solid Solution System

In the left-hand columns of Tables 2 and 3 the results of the Rietveld refinement of our $Li_{1.33}Ti_{1.66}O_4$ and $Li_{0.5}Fe_{2.5}O_4$ samples are compared with literature data. It is seen that good agreement is achieved.

For the Rietveld refinement of $Li_{0.5}Fe_{2.5}O_4$ and $Li_{1.33}Ti_{1.66}O_4$ we used literature data as starting parameters (17, 20). The site occupancy multipliers of the metal sites were included in the calculation. An overall temperature factor $B_{overall}$ was used in the refinement procedure since a calculation with individual isotropic temperature factors B_{iso} for each site did not reduce the residual R_{wp} value significantly (8.84 to 8.83 in the case of

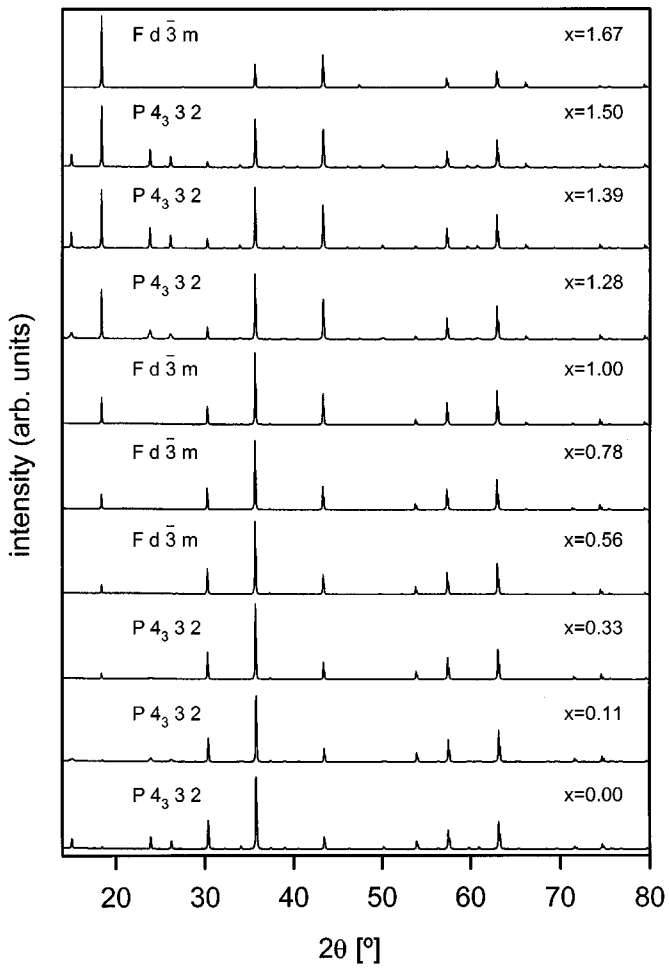

FIG. 4. XRD patterns (Cu$K\alpha$ radiation) of slowly cooled members of the $Li_{0.5+0.5x}Fe_{2.5-1.5x}Ti_xO_4$ solid solution system. The order–disorder transitions occur at $x = 0.4$, 1.2, and 1.57. Samples showing additional reflections belong to the space group $P4_332$.

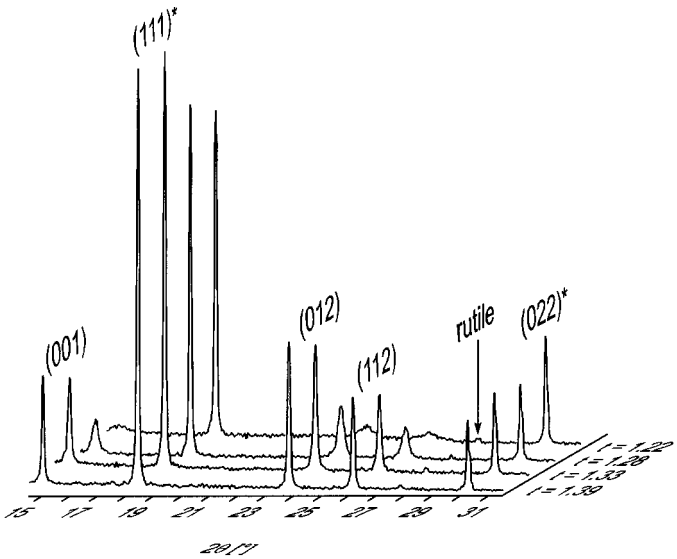

FIG. 5. XRD patterns (Cu$K\alpha$ radiation) of $Li_{0.5+0.5x}Fe_{2.5-1.5x}Ti_xO_4$ samples with $x = 1.39$, 1.33, 1.28, and 1.28. By approximation to the phase transition at $x = 1.2$ the intensity of the reflections typical for the space group $P4_332$ decreases and a strong line broadening is apparent. Reflections common to both space groups are represented by *.

$Li_{0.5}Fe_{2.5}O_4$). The calculated site occupancy multipliers for the metal sites reach the values for full occupancy with Li on octahedral sites (4*b*) and iron on octahedral (12*d*) sites and tetrahedral (8*c*) sites of the space group $P4_332$. Our $Li_{0.5}Fe_{2.5}O_4$ sample shows strong ordering of lithium and iron on the octahedral metal positions, which is in agreement with other results (17, 19).

In Table 3 the refined site occupancy multipliers of $Li_{1.33}Ti_{1.66}O_4$ in the second column indicate full lithium occupancy of the tetrahedral (8*a*) sites and mixed lithium–titanium occupancy of the octahedral (16*d*) sites.

In both cases, $Li_{1.33}Ti_{1.66}O_4$ and $Li_{0.5}Fe_{2.5}O_4$, our results are in good agreement with reported single-crystal data.

In order to calculate the site distribution of compounds along the $Li_{1.33}Ti_{1.66}O_4$–$Li_{0.5}Fe_{2.5}O_4$ join the scattering factors of the metal sites S_j were refined using the atomic scattering factor of Fe^{3+} for each site in the approximation of Eq. [6]. In this case the refined site occupancy multiplier of site j is denoted as C^j. A plot of the refined diffraction pattern of the solid solution $Li_{1.19}Fe_{0.42}Ti_{1.39}O_4$ is given in Fig. 7 with the calculated results presented in column 4 of Table 2. As can be seen by comparison of columns 2 and 3 of Tables 2 and 3, respectively, the approximation of Eq. [6] did not affect the structural parameters, such as atomic coordinates and the overall temperature factor. The site occupancy multiplier of lithium on position (4*b*) in $Li_{0.5}Fe_{2.5}O_4$ reduces from 0.142(4) to 0.0130(4) when the atomic scattering factor of Li^+ is replaced in the calculation by that of Fe^{3+}. The ratio $0.013/0.142 = 0.0915(4)$ is close to the value of $f_{Li^+}/f_{Fe^{3+}} = 0.088(1)$ (21).

In Fig. 8, the refined scattering factors S_j of the metal positions j are normalized to the scattering factor of a completely occupied by Fe^{3+} site

$$S_j^{\text{norm}} = S_j/(N^j \cdot f_{Fe^{3+}}) = C^j/N^j \qquad [16]$$

and plotted vs composition. In [16] N^j equals the multiplicity of site j divided by the multiplicity of the general position of the space group. The use of S_j^{norm} is advantageous since the site occupancy in different space groups symmetries can so be compared (Fig. 8).

In $Li_{0.5}Fe_{2.5}O_4$ the normalized scattering factors of the (12*d*) and (8*c*) sites approach unity as these sites are

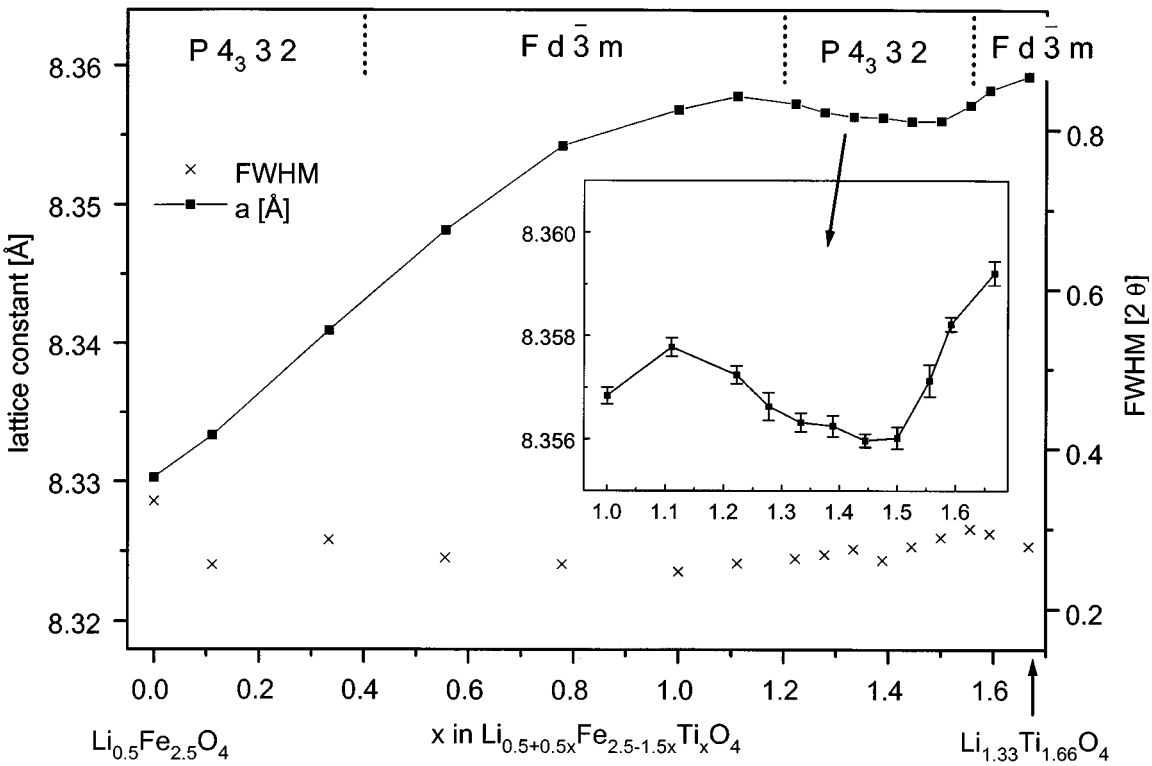

FIG. 6. Lattice parameter a and full width at half maximum (FWHM) of the (159) reflection of the $Li_{0.5+0.5x}Fe_{2.5-1.5x}Ti_xO_4$ solid solution members. This reflection is common to both space groups $Fd\bar{3}m$ and $P4_332$.

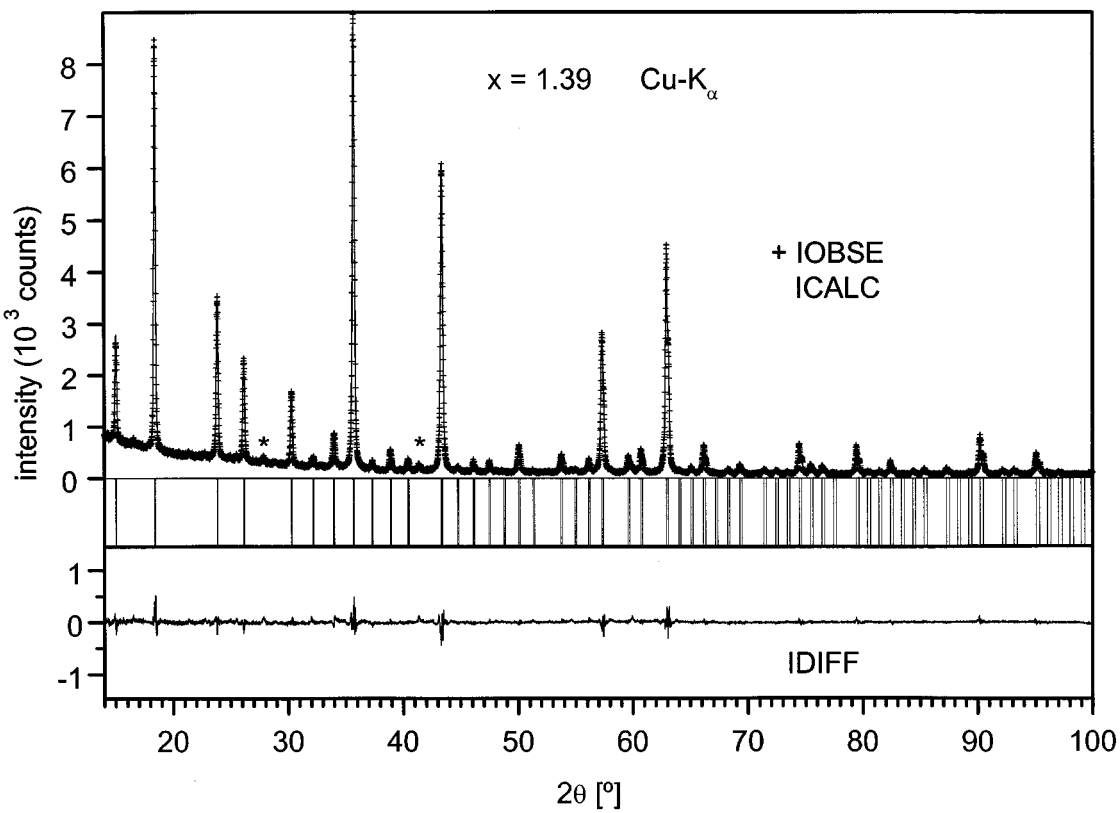

FIG. 7. Observed, calculated, and difference XRD patterns (Cu$K\alpha$ radiation) of $Li_{1.19}Fe_{0.42}Ti_{1.39}O_4$ (space group $P4_332$). (*) denotes traces of rutile.

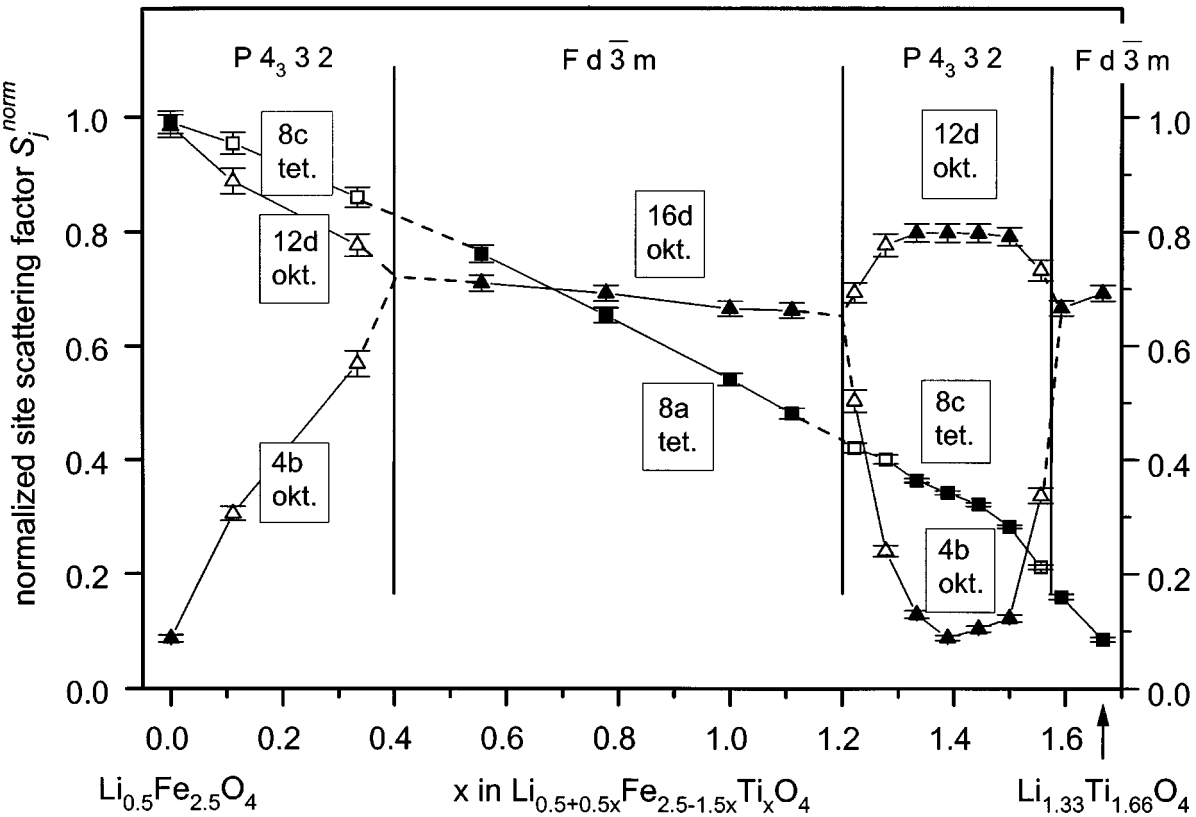

FIG. 8. Normalized scattering factors S_j^{norm} of the metal sites in the $Li_{0.5+0.5x}Fe_{2.5-1.5x}Ti_xO_4$ solid solution system. Open symbols represent samples in which the reflections typical of the space group $P4_332$ are broadened.

fully occupied by iron, whereas the normalized scattering factor of the (4*b*) site is 0.09 for complete lithium occupation.

In compounds with $0.4 \leq x \leq 1.2$ ($Fd\bar{3}m$) the octahedral metal sites are crystallographically equivalent. Accordingly, the S_j^{norm} value of the (12*d*) and (4*b*) sites converge when approaching this region. For compositions with $1.2 \leq x \leq 1.57$ the octahedral (16*d*) sites of space group $Fd\bar{3}m$ split up into the (12*d*) and (4*b*) positions of space group $P4_332$.

In $Li_{1.19}Fe_{0.42}Ti_{1.39}O_4$ S_j^{norm} of position (4*b*) crosses a minimum value which is equal to that for the lithium (8*a*) site in $Li_{1.33}Ti_{1.66}O_4$ and the lithium (4*b*) site in $Li_{0.5}Fe_{2.5}O_4$. This suggests that this position is fully occupied by lithium in the solid solution, also indicating a maximum order in the octahedral sublattice at this composition. The normalized scattering factor of the (12*d*) position remains nearly constant at 80% of a site fully occupied by iron. This suggests that this position is mainly occupied by titanium as the ratio of the atomic scattering factors of Ti^{4+} and Fe^{3+} is about 0.79 (Fig. 3). In the following we will demonstrate quantitatively that this picture is the only solution which agrees with the X-ray measurements. Physically reasonable cation distributions of the solid solution system were calculated according to the algorithm explained in a previous section. Because of the linear dependancy of Eqs. [7]–[15] the site occupancy multipliers $N_{Fe^{3+}}^{12d}$ and $N_{Fe^{3+}}^{8c}$ must be treated as variables and were varied between zero and the value for full occupancy.

From the calculated sets of solutions only those which included positive values for each site occupancy multiplier were plotted. The result for cationic site distribution is shown in Fig. 9. The fractional site occupancies for lithium, titanium, and iron are plotted versus the site occupancy of iron on (12*d*). In the range between 7 and 27% fractional site occupancy of Fe^{3+} on (12*d*) all the other fractional occupancies have positive values. Independent of other factors, a (4*b*) site completely occupied by lithium agrees with the X-ray data. Nonsignificant traces of iron and titanium have been calculated on this position. In contrast, the fractional occupancies of the (12*d*) and (8*c*) sites are much more variable. Iron and titanium can be completely exchanged on the tetrahedral position and any site distribution in the plotted graphs would agree with the measured X-ray diffractograms. Therefore, the exact cation distribution can only be determined with the help of other methods,

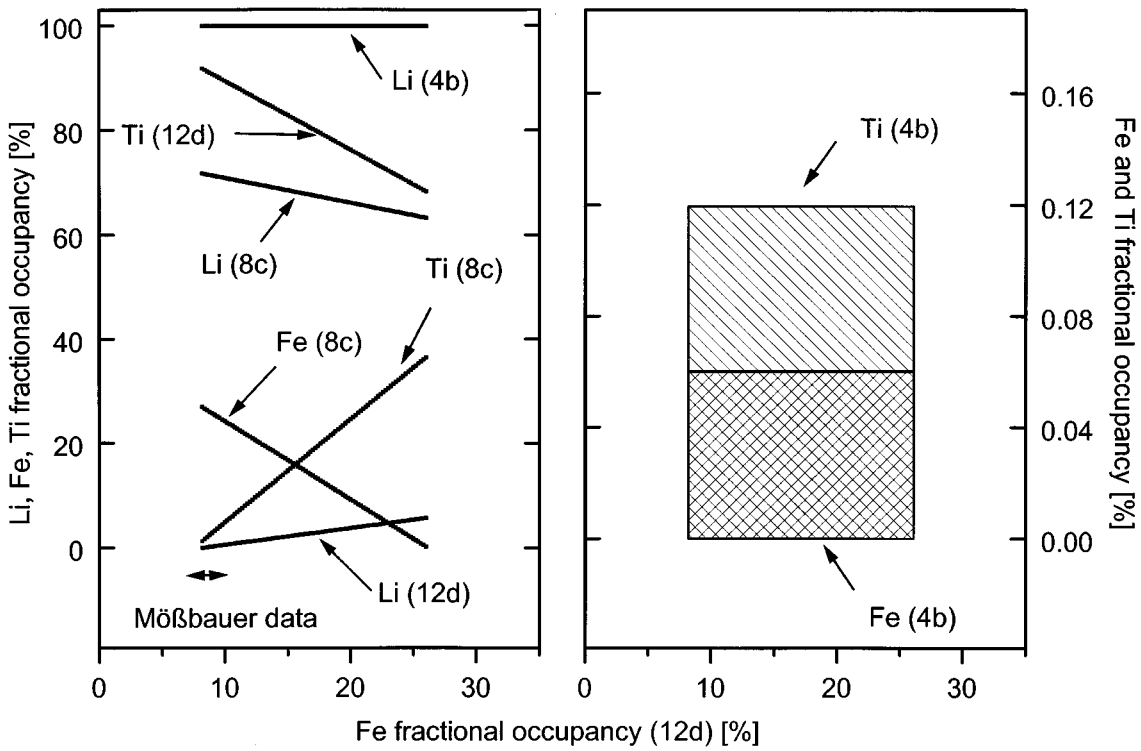

FIG. 9. Ranges of calculated fractional site occupancies of Li^+, Fe^{3+}, and Ti^{4+} in $Li_{1.19}Fe_{0.42}Ti_{1.39}O_4$ ($P4_332$). In agreement with the measured X-ray powder diffractions the (4*b*) site is almost completely occupied by Li^+. The ^{57}Fe-Mössbauer data (see Fig. 10) suggest that Ti^{4+} preferently occupies the octahedral (12*d*) site.

e.g. magnetic susceptibility measurements or Mössbauer spectroscopy.

Mössbauer Spectroscopy

^{57}Fe-Mössbauer spectra (Fig. 10) were recorded for the compositions: $x = 1.39$, 1.50, 1.56 (space group $P4_332$) and 1.59 (space group $Fd\bar{3}m$).

The diamagnetic spectrum of the spinel with $x = 1.39$ shows the same asymmetric line shape as recorded by Kishan *et al.* (12) for a sample with $x = 1.2$ (12). A weak shoulder on the high velocity side of the absorption line can be recognized. From $x = 1.39$ to $x = 1.56$ this asymmetry disappears and returns in the sample with $x = 1.59$ (space group $Fd\bar{3}m$).

Fitting the $x = 1.39$ sample resulted in two strongly overlapping subspectra. According to the literature, the expected value of the isomer shift of octahedral Fe^{3+} is more positive than that of the tetrahedral Fe^{3+} (19, 25). Consequently, and as lithium occupies (4*b*) sites, the more intense subspectrum in Fig. 10 ($x = 1.39$) must be attributed to tetrahedral Fe^{3+} (8*c*) and the other, which causes the asymmetric line shape, must be assigned to the octahedral Fe^{3+} (12*d*). A rough estimate of the integral absorption of the two subspectra of the $x = 1.39$ sample gives a ratio for A(Fe^{3+} tet)/A(Fe^{3+} oct) of 2.0(2). Assuming equal recoil-free fractions for $^{57}Fe^{3+}$ on both sites this result agrees with the iron site occupancies calculated from the diffraction data corresponding to a maximum content of Ti^{4+} on octahedral (12*d*) sites (Fig. 9).

Thus, the decreasing asymmetry of the spectra of the spinels with space group $P4_332$ is correlated with a decreasing occupancy of the octahedral (12*d*) position by iron. Following this argument, returning asymmetry of the sample with $x = 1.59$ ($Fd\bar{3}m$) shows that in the titanium-rich disordered spinels iron occupies the octahedral positions to a greater extent than in the ordered compounds with $1.2 \leq x \leq 1.57$.

Concerning the $x = 1.2$ spinel, it was argued that in spinels the cubic point symmetry of the tetrahedral site is maintained (12). With regard to the ordered compounds with compositions between $x = 1.39$ and 1.56 this argument cannot be used. The point symmetry of the (8*c*) site of the space group $P4_332$ is only 0.3 and an electric field gradient may arise, resulting in a quadrupolar split doublet (23).

Lattice Constants

Lattice constants of the $Li_{0.5+0.5x}Fe_{2.5-1.5x}Ti_xO_4$ solid solution system have already been reported by several

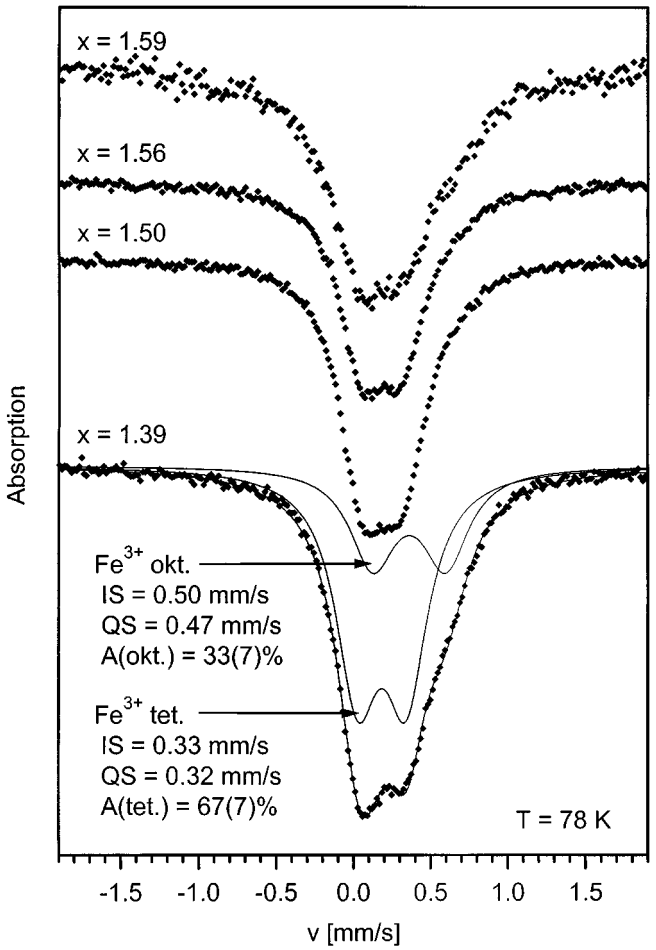

FIG. 10. ^{57}Fe-Mössbauer spectra at 78 K of $Li_{0.5+0.5x}Fe_{2.5-1.5x}Ti_xO_4$ solid solution members with $x = 1.39$, 1.50, 1.56 (space group $P4_332$) and $x = 1.59$ ($Fd\bar{3}m$): QS, quadrupole splitting; IS, isomer shift relative to α-Fe; A, integral absorption.

TABLE 4
Lattice Constants[a] of $Li_{0.5+0.5x}Fe_{2.5-1.5x}Ti_xO_4$[b]

x	a [Å]	N[c]
1.66[f]	8.3592(2)	19
1.59[f]	8.3582(2)	19
1.56[p]	8.3571(3)	32
1.50[p]	8.3560(2)	56
1.44[p]	8.3560(1)	54
1.39[p]	8.3563(2)	64
1.33[p]	8.3563(2)	54
1.28[p]	8.3566(3)	45
1.22[p]	8.3572(2)	26
1.11[f]	8.3578(2)	26
1.00[f]	8.3568(2)	26
0.78[f]	8.3542(2)	26
0.56[f]	8.3482(3)	27
0.33[p]	8.3409(2)	26
0.11[p]	8.3333(4)	39
0.00[p]	8.3303(2)	48

[a] With NBS 640 b as internal standard; errors as 3σ.
[b] Slowly cooled samples.
[c] Number of reflections used for the refinement; space group: [p] $P4_332$, [f] $Fd\bar{3}m$.

authors (5, 12, 13, 24). However, the precision of these data, especially of compounds with high titanium content, has remained poor. The X-ray diffractograms which have been used in this study cover a wide range from 15° to 160° in 2θ (Table 1). Therefore, much better resolution was achieved (Table 4 and Fig. 6). The unit-cell parameter a shows a sigmoidal dependency upon composition as found in spinels of the $FeCr_2O_4$ (chromite)–Fe_3O_4 (magnetite) join (25). In these compounds, the appearance of an inflection point is correlated with a rapid change of the cationic distribution. In contrast to this, in the spinel system $ZnFe_2O_4$ franklinite (normal)–Fe_3O_4 magnetite (inverse), the change of cationic distribution is constant with composition and a continuous development of the lattice parameter results (24). With respect to these considerations it seems reasonable that the compositional dependancy of the lattice constant in the $Li_{0.5+0.5x}Fe_{2.5-1.5x}Ti_xO_4$ system (Fig. 6) reflects a rapid change of the cationic site distribution due to an intracrystalline order process.

DISCUSSION

In order to determine an unequivocal cationic site distribution in our samples we repeated the site distribution calculations for each composition. We included our Mössbauer results for the titanium-rich samples and extended the observation that titanium prefers octahedral coordination over the whole compositional range of the spinel-type solid solution. Therefore, we extracted those calculated sets of solutions (Eqs. [7]–[13]) with the maximum possible Ti^{4+} content on octahedral sites and we present them in Fig. 11. With increasing x up to $x = 1.2$, iron and lithium are withdrawn from the octahedral sites at a nearly constant rate. Our data of the iron distribution fit the results of magnetic susceptibility measurements very well (5). The deviation of the lithium occupancy in our results may be due to the fact that the calucations in (5) were performed with a constant oxygen (32e) positional parameter. In the present study this variable was treated as a refinable parameter (Table 3). In the range between $x = 1.2$ and 1.57 a sudden drop of the molar ratio of octahedrally coordinated iron occurs. This is correlated with the inflection point in the lattice parameter plot (Fig. 6). In the same region the bump of the lithium curve reflects the ordering of lithium onto the octahedral (4b) site of the space group ($P4_332$), see Fig. 8. At the phase transition at $x = 1.57$ the amount of octahedrally

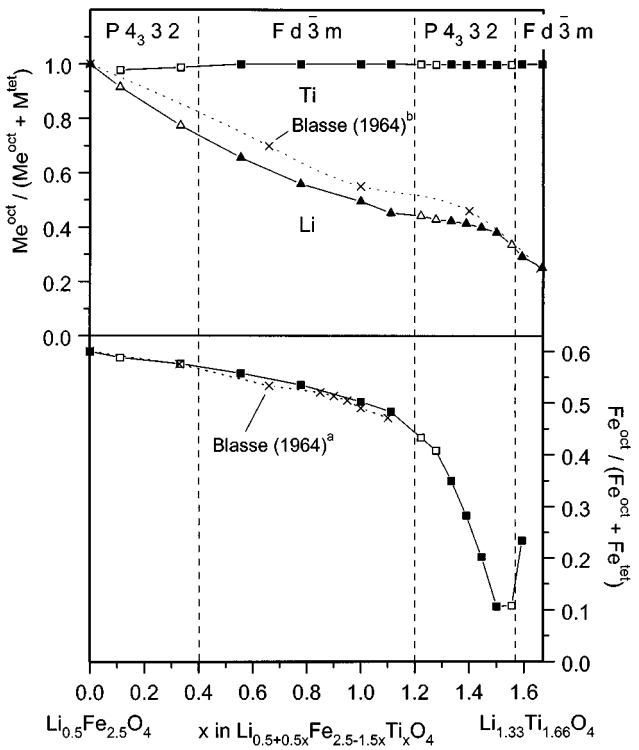

FIG. 11. Distribution of lithium, titanium, and iron over octahedral and tetrahedral sites in $Li_{0.5+0.5x}Fe_{2.5-1.5x}Ti_xO_4$. (solid lines) Calculated from X-ray data (this study); (open symbols) see Fig. 8; (dashed lines and crosses) from Blasse (5); [a] magnetic measurements, [b] X-ray diffraction measurements.

coordinated iron increases again and iron and lithium are redistributed over tetrahedral and octahedral sites. This interpretation agrees with the return of the asymmetry in the line shape of the Mössbauer spectrum of the spinel sample in Fig. 10 with $x = 1.59$.

SUMMARY

Several compounds of the spinel type system $Li_{0.5+0.5x}Fe_{2.5-1.5x}Ti_xO_4$ from $0 \le x \le 1.66$ were synthesized at 870°C in a pure oxygen atmosphere and slowly cooled. In contrast to most publications, our investigations cover the whole compositional range of this system with emphasis on titanium-rich samples. By analyzing the line width of the (159)-reflection, no miscibility gap was found as reported by Yau and Hughes for the iron-rich lithium titanium ferrite spinels below 755°C (24). This may be due to the higher reaction temperature of our samples with the kinetics being too slow to achieve equilibrium during cooling.

The lithium iron titanate spinel series exhibits three compositionally dependent phase transitions at $x = 0.4$, 1.2, and 1.57. Whithout the external assumption that titanium occupies octahedral sites we have shown that the phase transitions are a result of an order–disorder transition, where lithium prefers the octahedral (4*b*) positions of the space group $P4_332$. This process is reflected by the compositional dependancy of the lattice parameter *a* determined with high precision. The earlier presented model for the cation distribution from magnetic susceptibility measurements reported by Blasse (5) for iron-rich solid solution members was improved and extended to the titanium-rich side.

REFERENCES

1. E. Ferg, R. J. Gummow, A. de Kock, and M. M. Thackeray, *J. Electrochem. Soc.* **141,** L147 (1994).
2. T. Ohzuku, A. Ueda, and N. Yamamoto, *J. Electrochem. Soc.* **142,** 1431 (1995).
3. T. Ohzuku, A. Ueda, N. Yamamoto, and Y. Iwakoshi, *J. Power Sources* **54,** 99 (1995).
4. T. Gambke and B. Metz, *Glastechn. Ber.* **62,** 38 (1989).
5. G. Blasse, *Philips Res. Report Suppl.* **3,** 60 (1964).
6. G. O. White and C. E. Patton, *J. Magn. Magn. Mat.* **9,** 299 (1978).
7. M. Noguès, J. L. Dormann, M. Perrin, and W. Simonet, *IEEE Trans. Magn.* **6,** 1729 (1979).
8. J. L. Dormann, *Rev. Phys. Appl.* **15,** 1113 (1980).
9. J. L. Dormann, M. El Harfaoui, M. Noguès, and L. Jove, *J. Phys. C: Solid State Phys.* **20,** L161 (1987).
10. M. Krause, K. Knese, and P. Wartewig, *Hyperfine Interactions* **94,** 1839 (1994).
11. S. K. Kulshreshta, *J. Magn. Magn. Mater.* **53,** 345 (1986).
12. P. Kishan, C. Prakash, J. S. Baijal, and K. K. Larola, *Phys. Status Solidi* **84,** 535 (1984).
13. A. A. Yousif, M. E. Elzain, S. A. Mazen, H. H. Sutherland, M. H. Abdalla, and S. F. Masour, *J. Phys. Condens. Matter* **6,** 5717 (1994).
14. M. B. Reddy, V. D. Reddy, and P. V. Reddy, *Mod. Phys. Lett. B* **8,** 959 (1994).
15. M. B. Reddy, V. D. Reddy, V. N. Mulay, K. B. Reddy, and P. V. Reddy, *Mater. Sci. Eng. B* **22,** 201 (1994).
16. M. B. Reddy, V. N. Mulay, V. D. Reddy, and P. V. Reddy, *Mater. Sci. Eng. B* **14,** 63 (1992).
17. A. Tomas, P. Laruelle, J. L. Dormann, and M. Noguès, *Acta Crystallogr. C* **39,** 1615 (1983).
18. S. J. Marin, K. O'Keeffe, and D. E. Partin, *J. Solid State Chem.* **113,** 413 (1994).
19. J. L. Dormann, A. Tomas, and M. Noguès, *Phys. Status Solidi* **77,** 611 (1983).
20. A. Deschanvres, B. Raveau, and Z. Sekkal, *Mater. Res. Bull.* **6,** 699 (1971).
21. F. C. Hawthorne, *Am. Mineral.* **68,** 287 (1983).
22. R. A. Young, "The Rietveld Method." International Union of Crystallography, Oxford Univ. Press, 1995.
23. A. J. C. Wilson, Ed., "International Tables for Crystallography," Volume C. Kluwer Academic, Dordrecht, 1992.
24. Y. C. Yau and J. M. Hughes, *J. Am. Ceram. Soc.* **66,** 479 (1983).
25. C. P. Marshal and W. A. Dollase, *Am. Mineral.* **69,** 928 (1984).